Journal of Applied Electrochemistry **33**: 885–892, 2003.

Electrochemical treatment of wastewater containing phenolic compounds: oxidation at boron-doped diamond electrodes☆

A.M. POLCARO*, A. VACCA, S. PALMAS and M. MASCIA
Dipartimento di Ingegneria Chimica e Materiali, Università di Cagliari, Piazza d'Armi, 09123 Cagliari, Italy
*(*author for correspondence, e-mail: polcaro@dicm.unica.it)*

Received 29 October 2002; accepted in revised form 22 April 2003

Key words: BDD anodes, mass transfer, phenol oxidation, wastewater treatment

Abstract

This work investigates the performance of BDD electrodes during oxidation of aqueous solutions of phenol. The main reaction intermediates are identified, the effect of operating conditions on the faradic yield of the process, and the degree of mineralization achievable under different experimental conditions are evaluated. Due to the crucial role of mass transfer in the process, an impinging jet cell is used for the experiments. The results indicate that if a minimum value of current density is imposed, suitable initial conditions can be set at which the removal of the reactant is always under mass transfer control and the process is carried out at a faradic yield of about unity, up to the near-complete disappearance of total organic load. High current density and high mass transfer coefficient must be used in order to carry out the process with high space-time yield. The performance of BDD is compared to that obtained at Ti/RuO_2 anodes.

List of symbols

d	nozzle diameter (m)
h	distance between nozzle exit and electrode surface (m)
R	electrode radius (m)
V	volume of solution (m^3)
A	electrode area (m^2)
v	linear velocity in the nozzle (m s^{-1})
D_i	diffusivity of the ith compound (m^2 s^{-1})
ρ	density of electrolyte (kg m^3)
μ	viscosity of electrolyte (kg m^{-1} s^{-1})
C_i	concentration of the ith compound (mol m^{-3})
COD	chemical oxygen demand (mg dm^{-3})
TOC	total organic carbon (mg dm^{-3})
i	current density (A m^{-2})
i_{lim}	limiting current density (A m^{-2})
F	Faraday number (C mol^{-1})
t	reaction time (s)
k	specific reaction rate (m s^{-1})
k_m	mass transfer coefficient (m s^{-1})
Re	Reynolds number, $Re = vd\rho/\mu$
Sh	Sherwood number, $Sh = k_m d/D_i$
Sc	Schmidt number, $Sc = \mu/\rho D_i$
ε_F	Faradaic yield, $\varepsilon_F = \frac{V}{8}\frac{\Delta COD}{\Delta t}\frac{F}{iA}$
s	mean space time yield, $s = \frac{1}{t_f}\int_0^{t_f}\frac{1}{12}\frac{\partial TOC}{\partial t}dt$ (mmol s^{-1} dm^{-3})
r	mean oxidation rate $r = \frac{1}{t_f}\int_0^{t_f}\frac{1}{32}\frac{\partial COD}{\partial t}dt$ (mmol s^{-1} dm^{-3})

1. Introduction

Electrochemistry offers new and interesting approaches to industrial wastewater treatment: in particular, electrochemical combustion is a very attractive process for solutions in which, although the pollutant concentration is low, its presence makes the waste toxic [1].

Despite certain advantages, such as the versatility of the process and the simplicity of the reactors in terms of construction and management (which makes them particularly suitable for automation), the practical application of electrochemical techniques to wastewater treatment has been limited by the difficulty in finding anode materials with specific characteristics to make the process economically competitive. Several materials have been proposed as anode, such as Ti/PbO_2 [2], Ti/SnO_2 [3], Ti/IrO_2 [4] or glassy carbon [5] but some of these have shown loss of activity due to surface fouling (glassy carbon [6]) or limited service life (Ti/SnO_2 [7]).

A new electrode material has recently attracted attention because of its very promising characteristics [8, 9]: it consists of a silicon support coated by a layer of synthetic diamond, heavily doped with boron to obtain

☆ This paper was originally presented at the 6th European Symposium on Electrochemical Engineering, Düsseldorf, Germany, September 2002.

acceptable electrical conductivity. The characteristics of this material, such as hardness, stability up to high anodic potentials and the wide potential range over which discharge of water does not occur, make it an excellent candidate as anode in the oxidation of organic compounds [10].

Recent work has appeared demonstrating that complete combustion of organics can be achieved at high reaction rates when boron-doped diamond (BDD) electrodes are used as anodes in wastewater treatment: results show that mass transfer of the reactant to the anodic surface is the fundamental parameter for effective oxidation at this electrode [11].

This work focuses on the influence of mass transfer to the anode surface and of imposed current density on the faradaic yield and on the level of mineralization obtained during electrochemical oxidation at BDD of phenol, assumed as a model molecule representing a wide class of biorefractory compounds.

To improve the understanding of the system behaviour, oxidation of the main reaction intermediates was also performed.

Experimental runs were carried out in a batch electrochemical cell in which the solution was fed by a submerged nozzle which generates a solution jet perpendicular to the electrode surface. An accurate choice of suitable cell geometry enables the achievement of high mass transfer rates which can easily be modified by changing the electrolyte flow rate [12].

2. Experimental details

The cell used (Figure 1) was an impinging-jet electrode cell consisting of a section of Teflon pipe (10 cm high, 10 cm inner diameter). p-type semiconducting boron-doped diamond (boron concentration in the range 3500–5000 ppm), supplied by CESM, was used as anode ($R = 2.5$ cm). It was prepared by hot filament chemical vapour deposition (HFCVD) on a low resistivity silicon wafer (dia. 10 cm × thickness 0.5 cm).

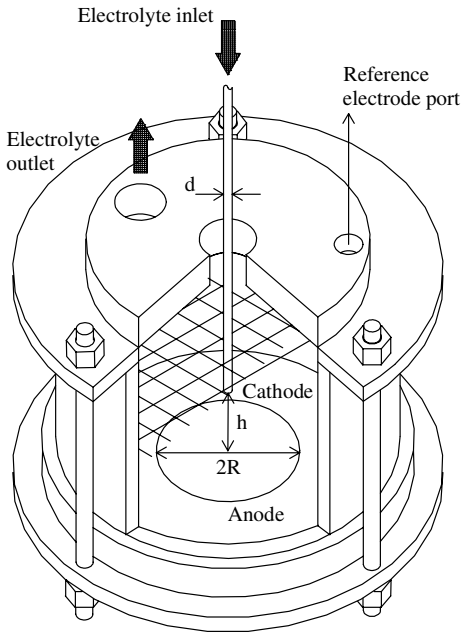

Fig. 1. Experimental cell.

The electrolyte jet was perpendicularly incident to the centre of the anode: the nozzle diameter (d) was 3 mm and the distance between the nozzle exit and the anode surface (h) was 2 cm. A grid of steel parallel to the anode and a saturated calomel electrode (SCE) constituted the cathode and the reference electrode, respectively.

The cell was inserted into a hydraulic circuit in which the electrolyte was pumped by a centrifugal pump from the reservoir to the cell and back in a closed loop. Flow rate ranged from 0.8 to 3 $cm^3\ s^{-1}$. The runs were carried out at constant temperature (25 °C) controlled by a heat exchanger also inserted in the hydraulic circuit.

Mass transfer in the cell was studied by oxidation of ferrocyanide ion solutions (0.1 M $K_3Fe(CN)_6$ + 1.5 × 10^{-3} M $K_4Fe(CN)_6$ + 0.5 M KNO_3). Oxidation of phenol as well as of hydroquinone, *p*-hydroxybenzoic and maleic acids was investigated by performing galvanostatic electrolyses of aqueous solutions in the initial concentration range between 100 and 500 ppm; perchloric acid was used as supporting electrolyte.

During oxidation, qualitative and quantitative analyses of parent compounds and the major intermediates originating from synthetic solutions were carried out by HPLC (UV detector (278 nm); column Chrompack Chromsphere 5 C8; mobile phase, CH_3OH + 0.1% H_3PO_4 and 0.05 M KH_2PO_4 + 0.1% H_3PO_4 = 50:50; flow rate 1.7 $cm^3\ min^{-1}$; column temperature, 25 °C). Identification of chromatographic peaks was performed by comparison with pure standards. The trend of oxidation was also monitored by measuring the chemical oxygen demand (*COD*) of the samples through a Merk SQ118 instrument, and the total organic carbon content (*TOC*) by a Shimatzu TOC 500A instrument.

3. Results and discussion

3.1. *Mass transfer study*

The impinging jet electrode is commonly used in electrochemical machining, erosion corrosion and other industrial processes. This configuration is known to be attractive as a means of intensifying convective processes, thus producing high local mass transfer rates [13]. The fluid dynamics and mass transfer characteristics of the impinging jet have been extensively studied [14–16]. To describe the dependence of mass transfer on the fluid properties, hydrodynamics and cell geometry, dimensional analysis has been used, leading to the following general expression:

$$Sh = lRe^m Sc^{1/3} \quad (1)$$

Table 1. Coefficient values in Equation 1: ($0.2 < H/d < 6$) [1]

R/d	l	m
2	0.342	0.59
3	0.133	0.68
4	0.0635	0.73
6	0.0316	0.77
8.3*	0.015	0.82

* This article.

where l and m depend on the cell geometry. Equation 1 is strictly valid only for values of the ratio between the radius of the electrode and the diameter of the nozzle (R/d) of less than 1, where the mass transfer coefficient (k_m) is independent of R; however, also in the 'wall jet' region ($R/d > 1$), where k_m depends on R, the same Equation 1 has been used, where k_m is considered as a mean value [17].

In the present case, to evaluate the dimensionless numbers involved in Equation 1, the physical properties of ferrocynide solutions (kinematic viscosity, $v = 0.952 \times 10^{-6}$ m^2 s^{-1} and diffusion coefficient, $D = 6.41 \times 10^{-10}$ m^2 s^{-1}) were used, the nozzle diameter d was adopted as characteristic length, while the mass transfer coefficient values at different flow conditions were derived by the following equation:

$$k_m = \frac{i_{lim}}{C_0 F} \tag{2}$$

where C_0 is the concentration of ferrocyanide ions and i_{lim} is the limiting current value obtained from the polarization curves for oxidation of ferrocyanide ions at different flow velocities.

The data, expressed in terms of *Sh* against *Re*, are well fitted by Equation 1 if values of l and m equal to 0.02 and 0.8, respectively, are used. These values are in agreement with data previously obtained in the turbulent regime for different cell geometries, as can be seen in Table 1 in which the l values decrease with the ratio between the radius of the electrode and the nozzle diameter. The m values also increase with R/d up to an asymptotic value of 0.8 [17].

3.2. *Kinetics of phenol removal*

Oxidation of phenol was performed by galvanostatic electrolyses with current densities ranging from 150 to 510 A m^{-2} and electrolyte flow rates corresponding to a range of *Re* between 3500 and 15000. Since it is well established that oxidative degradation of phenolic compounds at BDD electrodes only takes place in the potential region of O_2 evolution [11], the minimum value of applied current density was selected so that anodic potential higher than 2.7 V vs SCE was achieved, which corresponds to the minimum potential at which H_2O oxidation occurs.

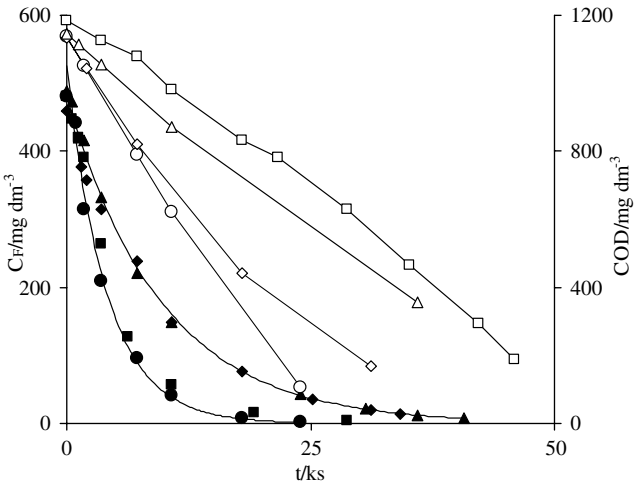

Fig. 2. Trend of phenol concentration (full symbols) and *COD* (empty symbols) as function of electrolysis time.(○ ●) $i = 305$ A m^{-2}, $Re = 13\,250$; (△ ▲) $i = 153$ A m^{-2}, $Re = 3500$; (□ ■) $i = 153$ A m^{-2}, $Re = 13\,250$; (◇ ◆) $i = 305$ A m^{-2}, $Re = 3500$.

Figure 2 shows the trend with time of phenol concentration (C_F) and chemical oxygen demand (*COD*) during electrolyses performed at different current density and electrolyte flow rate values. As can be observed, *COD* and C_F show different behaviour: the trend of phenol concentration is not affected by current density and it depends on the hydrodynamic conditions, whereas the trend of *COD* is influenced by current density and, to a lesser extent, by the flow rate.

Moreover, it was found that a linear trend with time of the logarithm of C_F is always followed, indicating first order kinetics:

$$\ln\left(\frac{C_F}{C_{F0}}\right) = -\left(\frac{A}{V}\right)kt \tag{3}$$

where C_{F0} is the initial concentration of reactant.

Table 2 shows the values of k obtained by linear regression of experimental data in the investigated range

Table 2. Values of specific reaction rate (k) under different experimental conditions for oxidation of phenol calculated by fitting of experimental data

C_0 /mg dm^{-3}	i /A m^{-2}	$q \times 10^5$ /m^3 s^{-1}	$k \times 10^5$ /m s^{-1}	R^2
97.9	153	2.97	11.60	0.980
241.3	305	2.97	12.42	0.990
416.3	510	1.10	3.76	0.999
437.4	510	2.97	12.74	0.997
460.1	153	0.78	2.64	0.998
464.6	305	1.40	5.00	0.999
479.7	153	2.97	9.17	0.991
481.2	305	2.97	11.45	0.999
481.3	510	2.97	12.81	0.995
482.7	305	0.78	2.11	0.978
488.8	153	1.40	5.25	0.999
497.0	153	2.97	7.98	0.986
528.0	510	1.90	8.72	0.997

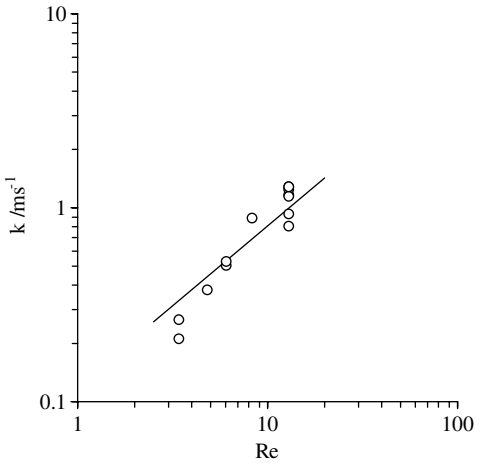

Fig. 3. Values of specific reaction rate (K) for phenol oxidation as a function of Reynolds number (Re); line calculated by Equation 1.

of current density and Re: the values of correlation coefficients, always greater than 0.98, confirm the good linearity of $\ln(C_F/C_{F0})$ against t obtained in all the examined conditions. Figure 3 shows a comparison between the k values and the mass transfer coefficients for phenol calculated for the relevant flux conditions using Equation 1 in which the physical properties of phenol solutions ($D = 8.1 \times 10^{-10}$ m^2 s^{-1} and $v = 1.04 \times 10^{-6}$ m^2 s^{-1}) were introduced: the satisfactory agreement indicates that k in Equation 3 actually represents the mass transfer coefficient of phenol to the electrode surface so, in all the examined conditions, the disappearance of the reactant may be assumed to be mass transfer controlled.

As was verified for COD removal, the trend of total organic carbon (TOC) during electrolyses of phenol solutions is also affected by both current density and electrolyte flow rate. Figure 4 shows the trend of mineralization ratio (TOC/TOC_0) as a function of removed phenol. As can be seen, removal of phenol being the same, the higher values of mineralization ratio are obtained at the lower flow velocities. When minimum current density and higher flow rates are used, the decrease in TOC is negligible up to the complete removal of phenol.

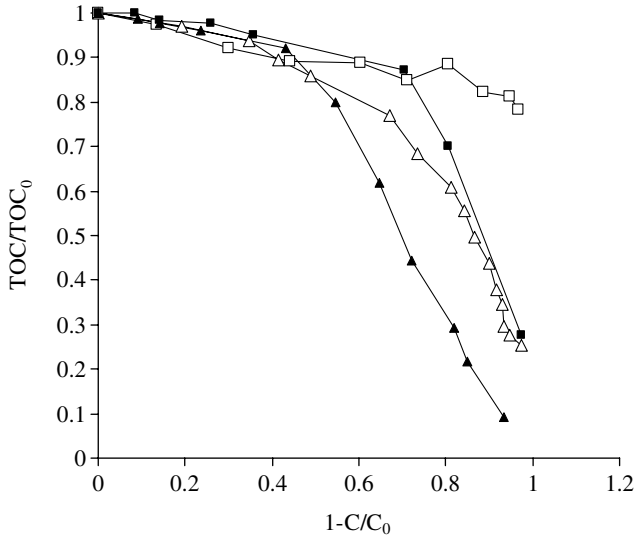

Fig. 4. Trend of total organic carbon (TOC) normalized with respect to its initial value as a function of the fraction of phenol removed during electrolyses under different experimental conditions: (□) $i = 153$ A m^{-2}, $Re = 13\,500$; (■) $i = 510$ A m^{-2}, $Re = 13\,500$; (△) $i = 153$ A m^{-2}, $Re = 4000$; (▲) $i = 510$ A m^{-2}, $Re = 4000$.

3.3. *Electrochemical behaviour of phenol oxidation by-products*

As already stated in the literature, in this case hydroquinone and benzoquinone have also been identified as main intermediates during the oxidative process. To explain the system behaviour, the degradation of these compounds was investigated under various experimental conditions. For these compounds oxidative degradation only occurs in the potential region corresponding to oxygen evolution, although some oxidation stages may be observed at less positive potential. Consecutive cyclic voltammograms are shown in Figure 5 for solutions of benzoquinone ($C_0 = 500$ ppm): an anodic current peak is observed at about 0.97 V vs SCE, the intensity of which decreases as the number of cycles increases. This decrease in the electrode activity is caused, as is also observed during oxidation of phenol at the same electrode [18], by the deposition of polymeric products on the electrode surface. However, in the range of imposed current in the present work, the anodic potential always shifted in the region of water decomposition and was constant during the runs: the decrease in TOC indicated that the oxidative degradation of benzoquinone, as well as of its intermediates, occurred without electrode deactivation.

However, unlike phenol, which during electrolysis disappeared under mass transfer control in all the examined conditions, the trend of disappearance of its intermediates is affected by both electrolyte flow rate and current density. Figure 6 illustrates the trend with time of the concentrations of hydroquinone, benzoquinone and maleic acid during electrolyses on BDD under different experimental conditions. The disappearance of hydroquinone occurs under mass transfer control only at the highest current density, whereas the reaction of benzoquinone and maleic acid is never controlled by diffusion: even at the highest current densities, the trend with time of $\log(C/C_0)$ is not linear and the rate of removal of the reactant is lower than that calculated on the basis of a mass transfer controlled process. This behaviour suggests that, experimental condition being equal, the oxidation rate of phenol is higher than that of the intermediates that are generated during oxidation of phenol itself.

The distribution of intermediates during degradation of phenol was investigated under different experimental conditions. Figure 7 shows some examples of the trend of the intermediate concentration as a function of the

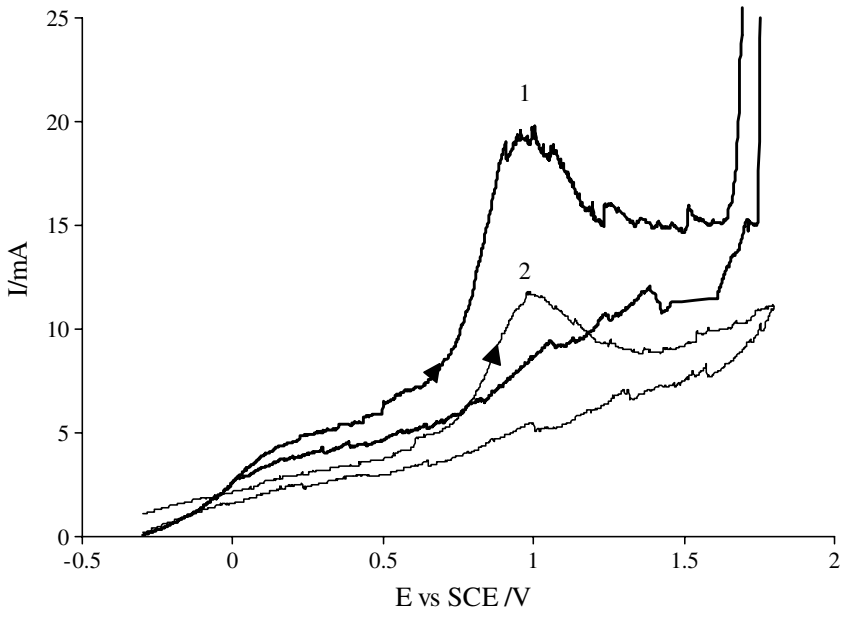

Fig. 5. Voltammograms related to consecutive cyclic voltammetries of 5 mM benzoquinone in 0.5 M sulfuric acid: scan rate 100 mV s^{-1}.

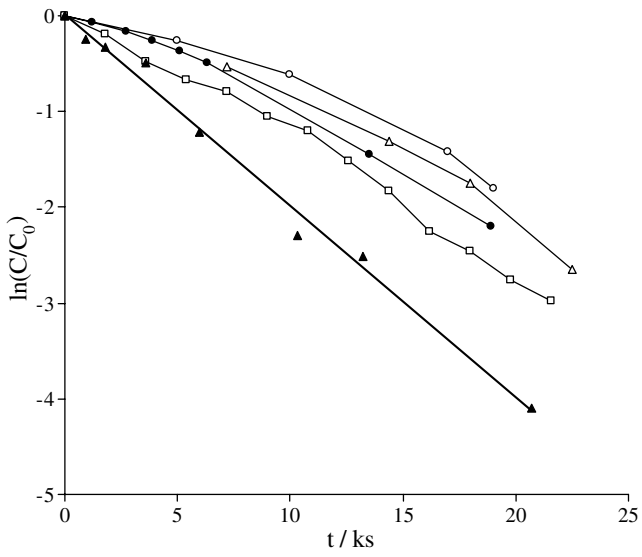

Fig. 6. Trend in time of benzoquinone (BQ), maleic Acid (MA) and hydroquinone (HQ) concentrations during electrolyses at $Re = 13\,000$ and different values of current density: (●) BQ, $i = 510$ A m^{-2}; (○) BQ, $i = 153$ A m^{-2}; (▲) HQ, $i = 510$ A m^{-2}; (△) HQ, $i = 153$ A m^{-2}; (□) MA, $i = 510$ A m^{-2}; straight line calculated by Equation 1.

ratio between the amount of electrical charge (Q) supplied to the system and the minimum amount (Q_T) for the complete mineralisation of phenol initially contained in the solution. The two extreme cases are identified: low current density ($i = 153$ A m^{-2}) and high flow rate ($Re = 13\,250$) enhance the accumulation of cyclic intermediates so that when 90% of phenol is removed, 66% of carbon in the solution consists of cyclic intermediates and only 10% of the initial carbon is mineralized; in the other extreme case, when the electrolysis is performed at high current density ($i = 510$ A m^{-2}) and low flow rate ($Re = 4000$), the products of oxidation detected when 90% of phenol is removed consist of a small amount of an aliphatic acid, and 93% of the initial carbon is converted to CO_2. These results are well supported by analogous information found in the literature. Iniesta et al. [11] found that at high current density ($i = 60$ mA cm^{-2}) and low concentration ($C_0 = 5$ mM), phenol was directly converted to CO_2 and H_2O under diffusion control. At lower current density ($i = 5$ mA cm^{-2}) and higher phenol concentration ($C_0 = 20$ mM), only a partial transformation of phenol to benzoquinone, hydroquinone and catechol was observed, but in this case the concentration of phenol decreased linearly with the specific charge. No information was given about the k_m values for the runs. During oxidation of phenol under different conditions, Canizares et al. [18] found that at $k_m = 2.83 \times 10^{-5}$ m s^{-1} and current densities in the range between 30 and 60 mA cm^{-2}, the main intermediates were carboxylic acids, namely maleic acid (C4 acids) and oxalic acid (C2 acids), whereas aromatic compounds (e.g., hydroquinone and benzoquinone) and other carboxylic acids (such as fumaric acid) were detected in low concentrations. The present work shows that different compositions of the solution can be observed during electrolyses if the operating conditions are varied between these two extreme cases (an example is depicted in Figure 7(b)).

3.4. *Effect of operating parameters*

An overall analysis of the data suggests that the distribution of intermediates, the percentage mineralization and the faradaic yield of the process only depend on the ratio γ between the imposed current density (i)

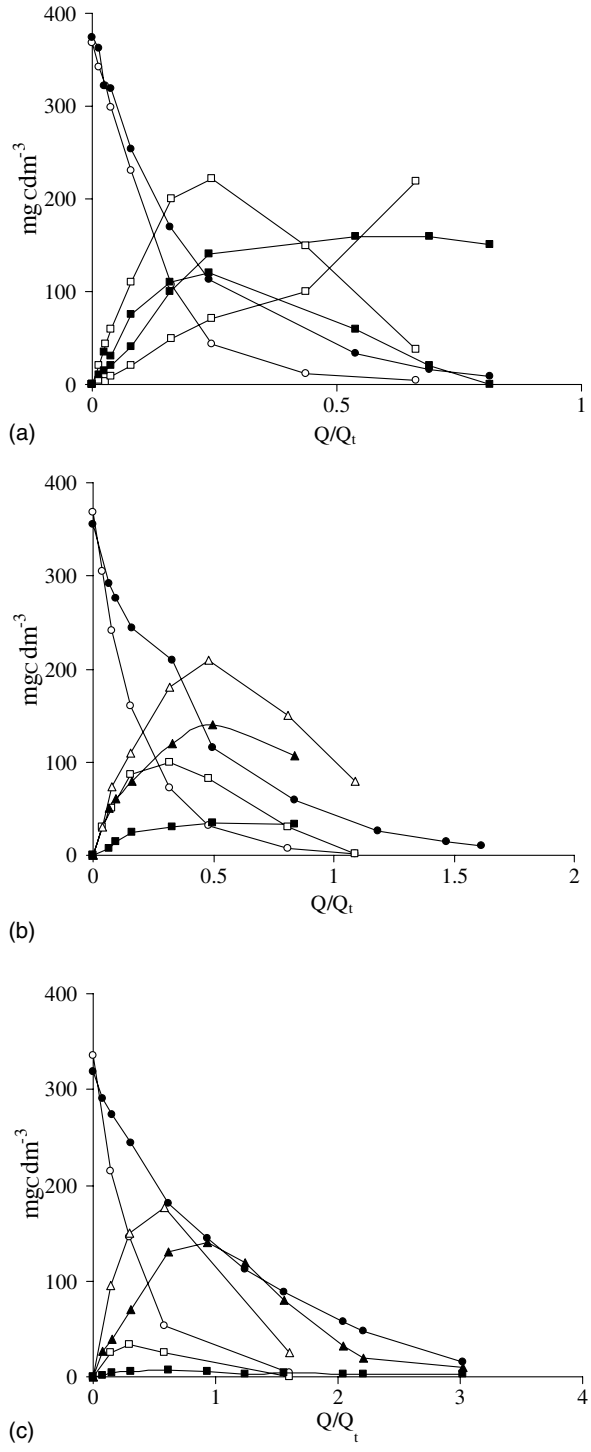

Fig. 7. Trend of concentrations (as equivalent mg of carbon) of phenol (● ○) cyclic intermediates (□ ■) and aliphatic acids (△ ▲) as a function of the ratio Q/Q_t. during electrolyses at $i = 153$ A m^{-2} (a), $i = 305$ A m^{-2}, (b), $i = 510$ A m^{-2} (c); full symbols $Re = 4000$; empty symbols $Re = 13\,500$.

and the initial value of limiting current density for the mineralization of phenol ($28\,Fk_mC_{F0}$), whatever the combination of experimental conditions which generate the particular γ value. Figure 8 shows the percentage of carbon present in solution as cyclic intermediates, as well as the percent of total organic carbon still present in

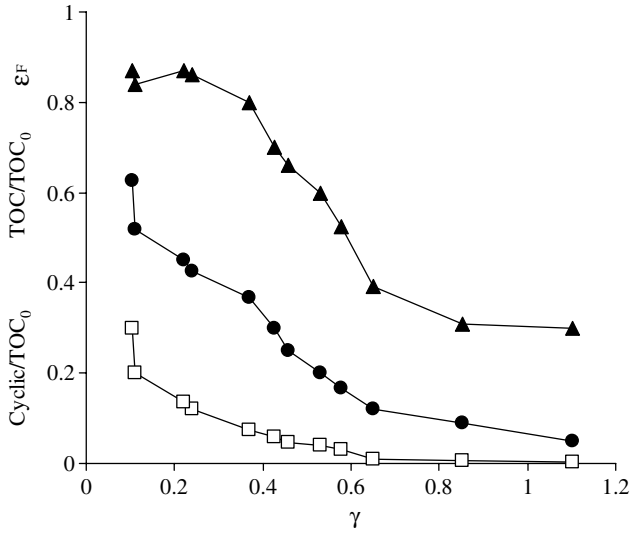

Fig. 8. Trend of *TOC* (●), dissolved carbon attributable to cyclic intermediates (□), both normalized with respect to TOC_0, and faradaic yield (▲) as a function of γ.

solution and the faradic yield (ε_F) as a function of γ: all these values are measured when 98% of phenol is removed from the solution. When γ is low, ε_F is almost unity, cyclic compounds constitute an appreciable fraction of the total carbon in solution and the mineralisation is low. In contrast, when γ approaches unity, the removal of phenol and its intermediates from the solution is achieved and ε_F is rather low. However, it is interesting to note that operating with $\gamma = 0.5$, when phenol is removed, partial mineralization is achieved; the residual compounds consist only of non toxic aliphatic acids, and the faradaic yield is still high. For particular values of γ, phenol removal occurs under diffusion control even if complete mineralisation is not achieved when the original reactant is removed from the solution.

To explain this behaviour, the kinetics of the process should be considered: electrode reactions may occur by direct electron transfer at the anode surface or, to a greater extent, by means of electrogenerated OH radicals [11, 18]. Since the oxidative reactions are in series with each other, but are in parallel with respect to the electrode reaction, the concentration of OH radicals in the reaction zone is determined by the fastest reaction step. As a consequence, if the initial flux of phenol to the electrode surface is high compared to that of OH radical generation, only the first step of the reaction is relevant. Therefore, a minimum value of current density ($i \geqslant 2Fk_mC_{0F}$, $\gamma \geqslant 0.07$, as was verified in all the examined conditions) must be imposed to allow the flux of OH radicals to complete the first oxidative step, of phenol to hydroquinone, which involves two electrons. In these conditions, the disappearance of phenol is mass transfer controlled and the concentration of OH is too low to provoke an appreciable reaction rate of the less oxidisable intermediates. Thus, the products of the first oxidative step accumulate in the laminar film, from

which they diffuse to the bulk solution where they are identified.

When higher values of γ are adopted for the electrolyses, from the initial reaction times the flux of OH is higher than that required for the first oxidative step and a greater amount of OH is available for the further steps. In these conditions, the presence of highly oxidized intermediates is experimentally revealed, and when the original reactant has disappeared from the solution, high mineralization is achieved. On the other hand, the high concentration of OH radicals enhances the production of O_2, so decreasing the faradic yield of the process.

3.5. *Application to phenolic wastewater treatment*

The results presented in this paper are useful for selecting the best process conditions for the electrochemical treatment of phenolic wastewater at BDD anodes. Depending on the aim of the process, different configurations have to be adopted and different figures of merit can be used to evaluate the performance of the treatment. However, the experimental results show that most of these figures of merit depend on γ.

If the aim of the process is the simple removal of the organic load, the faradaic yield evaluated when 90% of *TOC* is removed (ε_{90}) may be considered. The experimental results show that ε_{90} data can be correlated well ($R^2 = 0.98$) with γ by the following equation:

$$\ln(1 - \varepsilon_{90}) = 0.49\frac{1}{\gamma} \tag{4}$$

Equation 4 shows that to achieve good faradaic yield, low γ values must be guaranteed.

However, if the process specifications require that a high rate of organic removal be maintained during the process, ε_{90} is not an exhaustive parameter, and the mean space-time yield s should be considered; in the constant volume system adopted in the present case, s may be expressed as

$$s = \frac{1}{t_f}\int_0^{t_f}\frac{1}{12}\frac{\partial TOC}{\partial t}\,dt \tag{5}$$

where t_f is the electrolysis time at which 90% of *TOC* is removed from the solution.

Table 3 shows s values for runs at different k_m and current densities. This quantity s is independent of the current density at low k_m, while at higher k_m higher current densities allow increasing values of s to be obtained. Thus, the optimal operating conditions can be set if the low values of γ that are needed to obtain high faradaic yields are obtained using high current density and high mass transfer rates.

The organic removal could also be expressed as mean oxidation rate r, which is a useful parameter if the process is targeted at COD removal so that only partial mineralization is acceptable. If t_{f1} is defined as the electrolysis time at which 98% of phenol and cyclic intermediates are removed from the solution, the mean oxidation rate can be written as

$$r = \frac{1}{t_{f1}}\int_0^{t_{f1}}\frac{1}{32}\frac{\partial COD}{\partial t}\,dt \tag{6}$$

From the values of r reported in Table 3, it is evident that the optimal conditions, in terms of r, are also, in this case, achieved at low γ values.

If the aim of the process is to eliminate the toxicity of the waste, (i.e., to remove phenol and its cyclic intermediates, in particular benzoquinone, which is more toxic than phenol itself), the best operating conditions should allow the partial oxidation of phenol up to aliphatic acids.

Experimental results under different conditions show that the value of Q/Q_t required to remove 98% of toxic compounds from the solution (Q_{98}/Q_t) is a quantity linearly dependent on γ ($Q_{98}/Q_t = 3.43\ \gamma$, $R^2 = 0.92$): moreover, if the electrolysis is performed at low γ, the value of Q_{98}/Q_t is lower than that theoretically needed to fully remove the phenol from the solution and the process occurs with high faradaic yield.

A previous study carried out in our laboratory indicated that toxicity from solutions containing phenolic compounds can also be eliminated by electrochemical oxidation at Ti/RuO_2 anodes. At these DSA electrodes only partial oxidation of the reactant can be achieved: acceptable values of faradaic yield are obtained, provided that the presence of species (such as chlorides) able to react at the anode surface to give oxidizing agents is guaranteed in solution [4]. Table 3 shows a comparison between the performances of DSA and BDD electrodes in terms of mean oxidation rate (r). It can be observed that a good oxidation rate can also

Table 3. Values of s and r for runs under different experimental conditions

	$k_m \times 10^5$ /m s^{-1}	i /A m^{-2}	$s \times 10^5$ /mmol s^{-1} dm^{-3}	$r \times 10^5$ /mmol s^{-1} dm^{-3}
BDD anodes	9.98	153	5.53	63.37
		305	10.51	124.13
		510	14.24	206.60
	4.97	153	5.05	61.63
		305	6.74	79.86
		510	7.64	88.54
	2.01	153	4.20	43.40
		305	4.40	46.88
		510	4.53	48.61
DSA anodes	0.98	153	–	6.94
		305	–	9.55
		510	–	13.02
	0.11	153	–	26.04
		305	–	46.88
		510	–	104.17

be achieved at DSA electrodes but only at low mass transfer rates. In these conditions the performances of DSA are comparable with those obtained at BDD anodes at $i = 305$ A m^{-2} and $k_m = 9.98 \times 10^{-5}$ m s^{-1}.

As far as the consumption of current for the detoxification of the solution is concerned, we can compare the performances of two electrodes when both operate in the best conditions: we have experimentally observed that a value of Q_{98}/Q_t higher than that measured at BDD is obtained at DSA. However, a more correct comparison of two anodes should consider the molar consumption of energy rather than current:

$$W_{mol} = \frac{Q}{Q_t} 28 F E_{cell} \quad (7)$$

Although E_{cell} depends on the design of the cell, a lower E_{cell} value may be expected when DSA rather than BDD is used owing to the lower value of anode potential. At $i = 153$ A m^{-2} the working potentials were the following: $E_{an} > 1.2$ V vs SCE at DSA, and 2.7 V vs SCE at BDD. The lower cell voltage could compensate for the higher values of Q/Q_t and make the energy yields obtained with the two electrodes comparable.

Acknowledgement

This work was supported by the Italian Ministry of Research (L.488, INCA consortium).

References

1. K. Rajeshwar and J. Ibanez, 'Fundamentals and Applications in Pollution Abatement' (Academic Press, New York, 1997).
2. A.M. Polcaro, S. Palmas, F. Renoldi and M. Mascia, *J. Appl. Electrochem.* **29** (1999) 147.
3. Ch. Comninellis and C. Pulgarin, *J. Appl. Electrochem.* **23** (1993) 108.
4. A.M. Polcaro, M. Mascia, S. Palmas and A. Vacca, *Ind. Eng. Chem. Res.* **41** (2002) 2874.
5. A.M. Polcaro, S. Palmas, F. Renoldi and M. Mascia, *Electrochim. Acta* **46** (2000).
6. M. Gattrell and D.W. Kirk, *Can. J. Chem. Eng.* **68** (1990) 673.
7. B. Correa-Lozano, C. Comninellis and A. De Battisti, *J. Appl. Electrochem.* **27** (1997) 970.
8. F. Beck, H. Krohn, W. Kaiser, M. Fryda, C.P. Klages and L. Schafer, *Electrochim. Acta* **44** (1998) 525.
9. V. Fisher, D. Gandini, S. Laufer, E. Blank and Ch. Comninellis, *Electrochim. Acta* **44** (1998) 521.
10. M. Panizza, P.A. Michaud, G. Cerisola and Ch. Comninellis, *Electrochem. Commun.* **3** (2001) 336.
11. J. Iniesta, P.A. Michaud, M. Panizza, G. Cerisola, A. Aldaz and Ch. Comninellis, *Electrochim. Acta* **46** (2001) 3573.
12. O.A. Moreno, R.H. Katy, J.D. Jones and P.A. Moschak, *IBM J. Res. Devel.* **37** (1993) 143.
13. Y.M. Chen, W.T. Lee and S.J. Wu, *Heat Mass Transf.* **34** (1998) 195.
14. C.J. Chia, F. Giralt and O. Trass, *Ind. Eng. Chem. Fundam.* **16** (1977) 28.
15. F. Giralt and O. Trass, *Can. J. Chem. Eng.* **53** (1975) 505.
16. M.T. Scholtz and O. Trass, *AIChE J.* **16** (1970) 82.
17. D.T. Chin and C.H. Tsang, *J. Electrochem. Soc.* **125** (1978) 1461.
18. M.A. Rodrigo, P.A. Michaud, I. Duo, M. Panizza, G. Cerisola and Ch. Comninellis, *J. Electrochem. Soc.* **148** (2001) D60.
19. P. Canizares, M. Diaz, J.A. Dominguez, J. Garcia-Gomez and M.A. Rodrigo, *Ind. Eng. Chem. Res.* **41** (2002) 4187.